A Study of the Microstructural and Diffusion Properties of Poly(vinyl alcohol) Cryogels Containing Surfactant Supramolecular Aggregates

Annamaria Tedeschi,[†,‡] Finizia Auriemma,[†] Rosa Ricciardi,[†] Gaetano Mangiapia,[†,‡] Marco Trifuoggi,[†] Lorenzo Franco,[§] Claudio De Rosa,[†] Richard K. Heenan,[||] Luigi Paduano,[†,‡] and Gerardino D'Errico*[,†,‡]

Università di Napoli "Federico II", Dipartimento di Chimica, Via Cintia, I-80126 Napoli, Italy, Consorzio per lo Sviluppo dei Sistemi a Grande Interfase (CSGI), Italy, Università di Padova, Dipartimento di Scienze Chimiche, Via Marzolo, I-35131, Padova, Italy, ISIS Facility-CLRC, Rutherford Appleton Laboratory, Chilton, Oxon, OX11 0QX, United Kingdom

Received: March 29, 2006; In Final Form: September 8, 2006

Surfactant-containing poly(vinyl alcohol) (PVA) cryogels have been prepared by drying and reswelling hydrogel patches, previously obtained by the freeze/thaw procedure, in decyltrimethylammonium bromide (C_{10}TAB) aqueous solutions. The microstructural and diffusive properties of the resulting material have been characterized by a combined experimental strategy. Gravimetric measurements show that the cryogel maximum swelling is not affected by the surfactant. The surfactant concentration within the cryogel, measured by ion chromatography, is the same as that in the rehydrating surfactant solution. Electron paramagnetic resonance (EPR) spin-probe and small-angle neutron scattering (SANS) measurements show that surfactant self-aggregation in the gel is similar to that in water, occurring at the same critical concentration and resulting in the formation of micellar aggregates whose structure is not affected by the cryogel polymeric scaffold. However, both the micelle intradiffusion coefficients, measured by PGSE-NMR, and the spin-probe correlation times, measured by EPR, indicate that dynamic processes in the hydrogel are much slower than in bulk water. A quantitative analysis of these results suggests that the cryogel polymer-poor domains, in which surfactant molecules are solubilized, have an average dimension of ∼0.1 μm. Interestingly the experimental data also show that the polymer-poor phase contains more polymer than expected, suggesting that the spinodal decomposition, which occurs during the freezing step of cryogel preparation, is not complete or prevented by ice formation.

Introduction

In the past decade, a large amount of interest has been focused on the applications of hydrogels, i.e., polymer networks swollen by an aqueous medium, as devices for active delivery (e.g., in the pharmaceutical field) or for absorption of contaminants (e.g., for the treatment of polluted waters).[1−4]

Poly(vinyl alcohol) (PVA) hydrogels, being nontoxic and noncarcinogenic and presenting bioadhesive properties,[5−7] are particularly suitable in a large variety of biotechnological applications, for instance, in bioseparation chromatography or for immobilization of biomolecules and cells.[8−10] In addition, their use for biomedical applications is widely documented.[11,12]

PVA hydrogels can be prepared by different methods (e.g., exposure to radiation or addition of chemical cross-linkers) among which the freeze/thaw procedure has attracted much attention.[13] This method results in a physically cross-linked hydrogel, named cryogel, whose structure is imprinted by formation of ice crystals within a not yet structured water/PVA liquid mixture, during the freezing step. Ice crystals expel amorphous polymer segments, increasing the polymer concentration in the surrounding environment and inducing the formation of polymer microcrystallites.[14,15] Upon thawing the gel to room temperature, the ice crystals melt, but the gel structure does not collapse. During the successive cycles, the structure of the polymer scaffolding progressively improves and acquires a higher stability.

The freeze/thaw method for hydrogel preparation offers several advantages with respect to other methods, such as chemical or radiation-induced cross-linking: it is simple, does not require any additional chemical, which could reduce the hydrogel biocompatibility, and does not need high temperature. However, hydrogels obtained by the freeze/thaw procedure present a heterogeneous microstructure that is more complex than that of hydrogels obtained by other methods. In a generally accepted model, it may be described in terms of a porous polymer network composed of two separate phases, one with a low polymer concentration and the other with a high polymer concentration. The polymer-rich phase is segregated into closely interconnected regions and constitutes the macroscopic network. This network structure includes macropores, of the size of a micrometer,[16] filled by the polymer-poor phase, which is generally considered to be a very dilute polymer solution. The polymer-rich phase is itself organized and consists of an array of micropores, of the size of nanometers,[9,17] surrounded by a network of extensively solvated PVA polymer chains that are physically cross-linked by PVA microcrystallites.

* Corresponding author. E-mail: gerardino.derrico@unina.it. Telephone: +39 081674248. Fax: +39 081674090.
[†] Università di Napoli "Federico II".
[‡] Consorzio per lo Sviluppo dei Sistemi a Grande Interfase.
[§] Università di Padova.
[||] ISIS Facility-CLRC.

10.1021/jp061941m CCC: $33.50
Published on Web 10/18/2006

Control of the size of the different phases (polymer-poor and polymer-rich regions) and microphases (crystalline and amorphous regions) present in these gels and their relative arrangement is limited by the fact that these systems can show changes upon aging, even under controlled conditions that reduce water evaporation.[15−19] The negative effects of aging may be reduced by drying the freeze/thaw gel samples immediately after preparation and then restoring the gel to the swollen state when needed by rehydration of the dried gel samples.[15,18] It has been shown that the complex hierarchical structure at length scales of nano-[15] and micrometers[16] of these gels is not greatly altered upon drying and during the successive rehydration step; rehydrated gels, indeed, recover almost completely the volume, shape, and physical properties of the as-formed freeze/thaw PVA hydrogels.

The ability of freeze/thaw PVA hydrogels to include inside their porous network water soluble molecules of practically any size has been known for some time.[20] In a recent paper,[16] preliminary results were reported regarding the possible use of these gels to create devices for drug delivery containing both hydrophobic and hydrophilic domains by addition of sodium decyl sulfate micelles. To this aim, dried gel samples were swollen in aqueous solutions of sodium decyl sulfate, and the rehydrated gels characterized by small-angle neutron scattering (SANS) and electron paramagnetic resonance (EPR) measurements. When the concentration of sodium decyl sulfate in solution was higher than the critical micellar concentration (cmc), the molecules adsorbed in the gel matrix self-assembled into micelles of the same size as those formed in pure solvent. These micelles appeared not to be bound onto PVA chains, being free to move in the gel matrix; however, no quantitative data concerning their mobility was obtained. The diffusion of the micellar aggregates within freeze/thaw PVA hydrogels is a rather complex process due to the heterogeneous structure of the host matrix and has not been directly studied so far.

In this paper, we report the results of an experimental investigation on the self-aggregation process of the cationic surfactant decyltrimethylammonium bromide (C_{10}TAB) in physically cross-linked PVA cryogels. Both the microstructural aspects and the diffusive behavior of the system have been characterized. In this case, C_{10}TAB has been chosen as model surfactant because its NMR spectrum presents a strong, well-detectable peak (chemical shift = 3.2) due to the headgroup methyl groups, which can be easily followed for NMR measurements of diffusive properties. The aim of this study is 2-fold: from a basic viewpoint, the analysis of a process deeply dependent on the solvent properties, such as surfactant self-aggregation, leads itself to furnish detailed information on the medium in which it occurs. In other words, the behavior of C_{10}TAB molecules solubilized in the hydrogel pores reflects the properties of the swelling aqueous medium. Furthermore, the study of diffusion of C_{10}TAB micelles within the hydrogel could contribute to an understanding of aspects of the dynamics of other guest molecules, such as proteins. From an applicative viewpoint, addition of surfactants to hydrogel formulations, allowing the solubilization of hydrophobic compounds,[21,22] increases their possible applications, e.g., in drug delivery. In fact, the micelles formed by self-aggregation of surfactant molecules within the gels can be thought of as microcontainers for apolar guest molecules, while the hydrogel acts as a macrocontainer for the micellar system. In this connection, it is worth mentioning that C_{10}TAB, being an irritant, is not used as a carrier for pharmaceutical actives. Nevertheless, our results give a contribution to the general understanding of the micro-

CHART 1: Bond Structure of the Chemical Substances Used in the Present Work

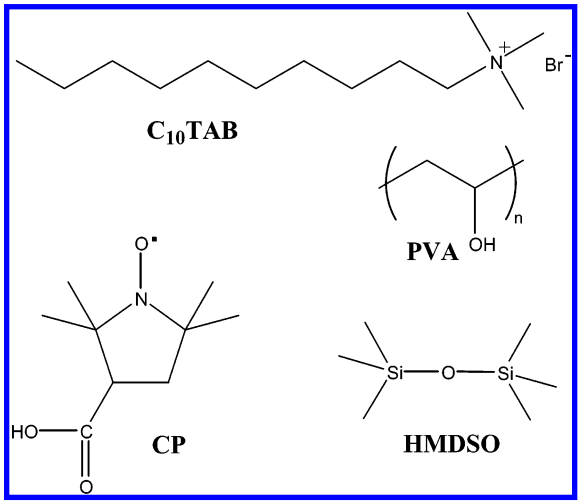

structural and diffusive properties of these systems, which could be useful for formulations using more suitable surfactants.

While surfactant self-aggregation in water and in dilute polymer solutions is a very well-known process,[23,24] much less attention has been paid to surfactant behavior inside a polymeric hydrogel. This is due to the fact that, for investigating these systems, many usual thermodynamic methods, e.g., tensiometry and calorimetry, are not suitable. In the present work C_{10}TAB self-aggregation in PVA hydrogel has been studied through: (i) EPR, employing the spin-probe 3-carboxy-PROXYL in its deprotonated form (CP^-); (ii) SANS; (iii) ^{1}H pulsed gradient spin−echo (PGSE) NMR. These nondestructive techniques are shown to be suitable for an in situ characterization of the surfactant self-aggregation in hydrogels. As a preliminary part of the investigation, the maximum swelling of PVA hydrogel in C_{10}TAB solutions was measured, and an analytical method was developed for the determination of the C_{10}TAB concentration inside the hydrogel based on ion exchange chromatography.

Experimental Section

Materials. The surfactant decyltrimethylammonium bromide ($CH_3(CH_2)_9N(CH_3)_3Br$, C_{10}TAB, purity > 98%) was purchased from Fluka. Commercial grade poly(vinyl alcohol) (PVA), with an average molecular weight, $\bar{M}_w$, of about 115 000 and a degree of hydrolysis of 98−99%, was purchased from Aldrich. For the gravimetric and chromatographic measurements, doubly distilled and degassed water was used as solvent. For hydrogel preparation, as well as for EPR, SANS, and PGSE-NMR measurements, heavy water (Sigma-Aldrich, purity > 99.8%) was used. 3-Carboxy-PROXYL (2,2,5,5-tetramethyl-3-carboxy-pyrrolidinyloxy, CP), used as a spin-probe in EPR measurements, and hexamethyldisiloxane (HMDSO, purity >99.5%), used as a micellar probe in PGSE-NMR measurements, were purchased from Aldrich. All chemicals were used without further purification. The molecular formulas of the chemical substances are shown in Chart 1.

Preparation of PVA Hydrogel Samples Containing C_{10}TAB. The PVA hydrogel was prepared through the freeze/thaw procedure.[13−20] An aqueous solution of PVA at 11% w/w was prepared by dissolving the PVA polymer in heavy water at 96 °C, under reflux and stirring, for about 3 h. The homogeneous solution obtained was slowly cooled to room temperature and kept at this temperature for one night to eliminate air bubbles. The aqueous PVA solution was then poured between glass slides

with 1 mm spacers, and subjected to three repeated freeze/thaw cycles, consisting of a 20 h freezing step at −22 °C followed by a 4 h thawing step at 25 °C. As discussed elsewhere,[19] three cycles are enough to obtain hydrogel samples with good mechanical properties. The hydrogel was then dried, leaving the samples in air, at room temperature, up to obtain a constant weight (residual water content ∼9% w/w). These dried samples keep the capability to rehydrate when put in water.[15,18] To obtain surfactant-containing hydrogels, patches of a dried hydrogel sheet (approximately 1 × 1 cm^2) were rehydrated, for 24 h at 25 °C, by placing them into screw-cap vials containing a large excess (∼5 cm^3) of C_{10}TAB aqueous solutions at concentrations ranging between 0.006 and 0.276 mol kg^{-1}. Once swollen, the hydrogel patches maintain good mechanical properties[19] and can be easily removed from the surfactant solution and superficially dried with filter paper.

Gravimetric Measurements. The amount of aqueous surfactant solution taken up by the dried hydrogel was determined by weighing, using a Mettler AT400 analytical balance (readability and reproducibility equal to 0.1 mg), each hydrogel patch before and after the rehydration procedure described above.

Chromatography Measurements. The C_{10}TAB concentrations in the same hydrogel samples used for gravimetric measurements were determined via ion chromatography measurements of the bromide concentration.[25] PVA solutions and hydrogels were previously checked to be free from bromide impurities. The bromide concentration in each hydrogel patch swollen in C_{10}TAB solution was determined and compared to the value for the corresponding rehydrating C_{10}TAB solution. The hydrogel patches removed from the C_{10}TAB solutions were weighed, transferred in beakers containing doubly distilled water, and heated at 90 °C for 3 h to melt the PVA crystallites, causing the breaking of the hydrogel structure. The resulting viscous solutions were diluted, degassed by applying vacuum for at least 10 min, microfiltered (0.45 μm filter), and then analyzed for bromide concentration. A Metrohm IC761 ion chromatograph equipped with a conductivity detector was used. Loop volume was 20 mm^3. The separation column was a Metrohm METROSEP ANION DUAL1 (length 150 mm), containing spherical particles (size 10 μm) of hydroxyethyl methacrylate derivatized with quaternary ammonium groups, used with chemical suppression of conductivity; the column was preceded by a column guard (Metrohm METROSEP ANION DUAL1 GUARD) made of the same material. A standard carbonate eluent (2.4 mM sodium hydrogen carbonate, 2.5 mM sodium carbonate) was used, adding 2% acetonitrile to prevent bacterial growth. Standard flow of 0.5 cm^3/min (pressure 3.0 MPa) was adopted to separate with good resolution inorganic anions, from fluoride to sulfate, in ca. 16 min.

Bromide concentration in the samples was determined by measuring the area of the corresponding peak in the chromatogram (elution time ∼10 min). A linear calibration graph was previously obtained employing a series of standard solutions; working standards were prepared daily by appropriate dilution of a certified stock solution (ROMIL Ltd, Cambridge, concentration 1000 ppm) with doubly distilled water. The reproducibility of bromide concentration for a particular sample was in the range 1−2%, depending on the absolute bromide content. Selected samples were checked with an independent method of analysis based on bromide titration, obtaining good agreement (deviation < 2%) with chromatographic data.

EPR Measurements. A stock solution of the spin-probe CP in heavy water (1.0×10^{-4} mol kg^{-1}) was prepared by weight. Heavy water was used as solvent to allow a direct comparison between EPR, SANS, and PGSE-NMR measurements. The pH was adjusted to 7.0 by adding small quantities of concentrated aqueous sodium hydroxide. The pH was measured through a Radiometer pH-meter, model PHM240, equipped with a double-junction reference electrode. At pH = 7.0, the carboxylic group of CP ($pK_a = 4.0$) is almost completely deprotonated,[26] and the deprotonated species CP^- is responsible for the EPR signal. The CP^- solution was used as a solvent for preparing C_{10}TAB solutions at surfactant concentrations between 0.017 and 0.962 mol kg^{-1}. In turn, these solutions, after degassing by prolonged bubbling with pure nitrogen, were used as a swelling medium to rehydrate, for 24 h at 25 °C, patches of dried hydrogel.

To execute the EPR measurements, small portions of these rehydrated PVA patches were cut (approximately 0.3 cm × 0.5 cm) and put on a plane plastic holder (5 mm wide), which could be inserted in the center of a TM_{110} cylindrical cavity. The spectra were recorded at 25 °C with a Bruker ER200D spectrometer.

For comparison, EPR measurements were performed on CP^- (1.0×10^{-4} mol kg^{-1}) in liquid mixtures of heavy water−PVA at polymer concentrations between 1 and 18% w/w. These samples were prepared using the CP^- solution as solvent.

EPR measurements were also performed on CP^- (1.0×10^{-4} mol kg^{-1}) in liquid mixtures heavy water−C_{10}TAB−PVA (1% w/w) at various surfactant molalities. In this case, the samples were prepared as follows: the CP^- solution in heavy water was used for preparing a PVA solution at 1% w/w. This solution, in turn, was used as a solvent for preparing the samples at various C_{10}TAB molalities. The samples were degassed and put in capillary quartz tubes (0.5 mm i.d.) for the EPR measurements. For liquid mixtures, the EPR spectra were recorded with the same spectrometer as above, but using a TE_{011} cavity.

SANS Measurements. SANS measurements were performed on the LOQ instrument at the ISIS Facility, Rutherford Appleton Laboratory. SANS measurements on PVA hydrogels have also been performed at the KWS2 instrument at the FRJ-2 reactor located in Jülich and are in agreement with those reported here. Such measurements have been presented in ref 16. ISIS is a pulsed neutron source, and thus, LOQ is a time-of-flight instrument that, operating at 50 Hz, uses neutrons with wavelengths $2.2 < \lambda < 10$ Å to give a wave vector transfer $0.006 < Q < 0.284$ $Å^{-1}$ on its main detector located 4.1 m from the sample, where $Q = (4\pi/\lambda)\sin(\theta)$, and 2θ is the scattering angle.

Samples were prepared by weight using heavy water as solvent to enhance the scattering contrast and minimize incoherent background from hydrogen atoms. All liquid samples were placed in 1 mm path length Hellma quartz cells, whereas the PVA hydrogels rehydrated in heavy water−C_{10}TAB solutions were wrapped in an aluminum foil and placed in the sample rack; measurements were performed at 25 °C. The time-of-flight data were corrected for the wavelength-dependent monitor spectrum, sample transmission, and detector efficiency. Background scattering was removed by subtraction of scattering from either heavy water or an empty foil packet. Residual incoherent background scattering from the samples was treated as a flat background term in all fits. The differential scattering cross section data, $d\sum/d\Omega$, were normalized to an absolute scale by reference to scattering from a standard sample (a solid blend of protonated and deuterated polystyrene) with a known differential scattering cross section.[27]

^{1}H PGSE-NMR Measurements. C_{10}TAB intradiffusion coefficients in PVA hydrogel patches rehydrated in heavy water−surfactant mixtures were measured by the ^{1}H PGSE-

TABLE 1: Total Weight Percentages of Water−C_{10}TAB Solution in the Swollen PVA Hydrogel, w_w; C_{10}TAB Concentrations in Rehydrating Solution and the Swollen hydrogel patches at 25 °C

w_w (% w/w)	$m_{C_{10}TAB}$[a] (mol kg^{-1})	$m_{C_{10}TAB}$[b] (mol kg^{-1})
78[c]	0.000	
77	0.006	0.007
78	0.036	0.037
79	0.105	0.109
80	0.129	0.123
79	0.276	0.264

[a] Stoichiometric molality of rehydrating C_{10}TAB solutions. [b] Molality of C_{10}TAB in the hydrogel patches measured by ion chromatography. [c] Datum from ref 15.

NMR technique.[28] Surfactant concentrations between 0.504 and 1.179 mol kg^{-1} were considered. For comparison, intradiffusion coefficients of C_{10}TAB in heavy water and in heavy water−PVA liquid mixtures were also determined. Heavy water was used as a solvent for NMR field/frequency lock purposes and in order to enhance the surfactant NMR signals. Experiments were carried out on a Varian FT 80 NMR spectrometer operating in the ^{1}H mode, equipped with a pulsed magnetic field gradient unit, specially made by Stelar (Mede, Italy).

The stimulated spin−echo sequence was employed. If only one kind of diffusing molecule gives rise to the NMR signal, the quantitative relationship between the attenuation of the echo intensity and the intradiffusion coefficient is given by:

$$I = I_0 \exp\left[- D_i \gamma^2 G^2 \delta^2 \left(\Delta - \frac{\delta}{3} \right) \right] \quad (1)$$

where D_i stands for the intradiffusion coefficient of the *i*-species responsible for the NMR signal, and γ for the gyromagnetic ratio of the ^{1}H nucleus. δ and G are the duration and the strength of the magnetic field gradients, while Δ is the duration between the onsets of the gradients. I and I_0 are the spin−echo signal intensity with and without gradients, respectively. If more than one kind of diffusing molecule gives rise to an NMR signal, eq 1 does not hold and a multiexponential decay is usually observed. ^{1}H PGSE-NMR experiments were performed by varying the gradient strength, G, from 0 to 0.02 T m^{-1} and keeping all timing parameters constant ($\Delta = 0.10$ s, $\delta = 0.02$ s). The intradiffusion coefficient, D_i was determined by an appropriate nonlinear least-squares analysis of the data through eq 1. Each measure was repeated at least three times on the same sample, obtaining intradiffusion coefficient values with a standard deviation lower than 2%.

Results and Discussion

Gravimetric and Chromatography Data. The maximum swelling reached during rehydration of PVA hydrogel patches in water−C_{10}TAB solution was determined by gravimetric measurements with concentrations of C_{10}TAB both above and below its cmc (0.06 mol kg^{-1}, see below). The weight percentages of water−C_{10}TAB solution in the completely swollen PVA hydrogel patches, w_w, are shown in Table 1, together with a datum for the surfactant-free sample, taken from a previous study.[15] Inspection of the table shows that the hydrogel maximum swelling is not affected by addition of surfactant to rehydrating water and is independent of surfactant concentration. This evidence suggests that the polymeric matrix is unperturbed by the presence of surfactant molecules, both in monomeric and in micellized form, in the swelling medium. For selected samples, longer rehydration times (up to 3 days) showed no significant variation in the results.

The C_{10}TAB concentration in the rehydrated hydrogel patches is also reported in Table 1. These concentrations, measured by ion chromatography, are the same as that in the rehydrating surfactant solution, indicating no surfactant preference for the hydrogel, thus suggesting that no chemical interaction takes place between the surfactant and the polymeric matrix.

EPR Data. EPR measurements need the introduction of a paramagnetic molecular spin-probe in the investigated system. The cyclic nitroxides are particularly suitable as probes because they are remarkably stable and can be tailored to solubilize in the microdomain of interest.[29−33] Information about the local physicochemical properties of the solubilization site is obtained from analysis of the spin-probe isotropic nitrogen hyperfine coupling constant (A_N) and correlation time (τ_C). A_N depends on the polarity of the medium in which the nitroxide is embedded; in particular, its value increases with both the solvent polarity and H-bonding ability. At the same time, τ_C clearly shows changes in the probe rotational mobility, as determined by the microenvironment viscosity and/or by specific interactions.

3-Carboxy-PROXYL in its deprotonated form, CP^-, has been already successfully employed as spin-probe to characterize the micellization process of alkyltrimethylammonium bromides (C_nTAB) in water.[34] A quantitative analysis of the experimental results is made possible by a previous experimental and computational study on the factors affecting the EPR spectral parameters of CP^-.[26] In the present study, this probe is used to characterize the micellization of C_{10}TAB in PVA hydrogel. Initially, the effect of PVA on the CP^- spectroscopic parameters was studied in the absence of surfactant, both in liquid solution and in hydrogel. All the CP^- EPR spectra showed the typical triplet of narrow lines due to hyperfine coupling of the unpaired electron with the ^{14}N nucleus. The narrow line width (approximately 1 G, see Figure 1), indicates a fast isotropic tumbling of the spin-probe. According to the classical theory of motional narrowing of EPR lines,[35] the nuclear spin state dependence of the width of the hyperfine line of a nitroxide, ΔB, is described by the formula:

$$\Delta B(m_I) = A + Bm_I + Cm_I^2 \quad (2)$$

where m_I is the nitrogen nuclear spin quantum number. As described in a previous work,[34] the values of *A*, *B*, and *C* were determined by means of a least-squares fitting routine of experimental spectra using eq 2. In turn, their values allow calculation of the isotropic nitrogen hyperfine coupling constant, A_N, and the tumbling correlation time of the spin-probe, τ_C. The precision of τ_C values is about 10%, while the experimental error on A_N values is estimated to be about 0.02 G.

The same values for A_N and τ_C of CP^- (1.0×10^{-4} mol kg^{-1}) were found in heavy water and in a diluted PVA aqueous solution (1% w/w), see Table 2, indicating that no direct probe−polymer interaction takes place. With further increasing of PVA percentage, τ_C increases as a result of the increased viscosity of the solution. The EPR spectrum was also measured on a PVA hydrogel patch rehydrated for 24 h at 25 °C in a heavy water solution of CP^-; the PVA content in the hydrogel was 22% w/w. The A_N and τ_C values obtained are reported in Table 2 and shown in Figure 2. Overall, the polymer gelation effect on the CP^- EPR parameters is low, confirming reports in the literature for other nitroxides.[36,37] Inspection of Table 2 shows that A_N remains almost constant, within the experimental error, while τ_C is lower than expected for a liquid solution at the same

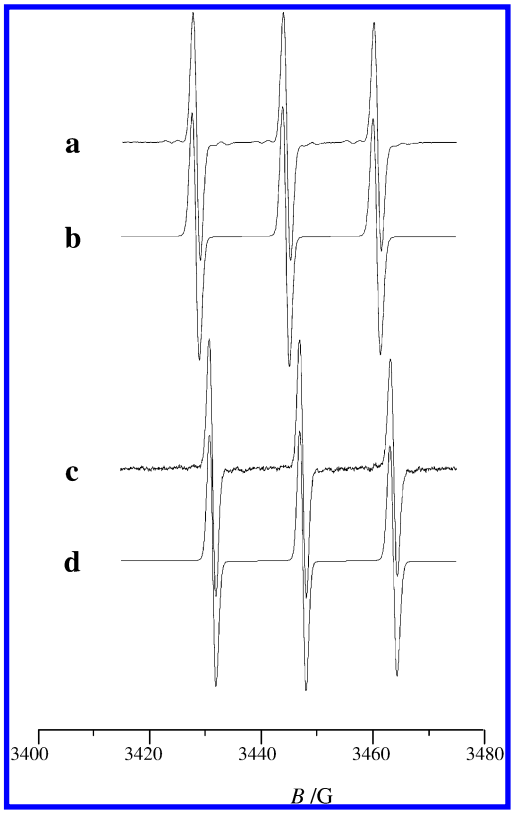

Figure 1. CP^- EPR experimental (a) and simulated (b) spectrum in heavy water−C_{10}TAB−PVA (1% w/w) solution ($m_{C_{10}TAB} = 0.0430$ mol kg^{-1}) at 25 °C. CP^- EPR experimental (c) and simulated (d) spectrum in PVA hydrogel swollen in heavy water−C_{10}TAB solution ($m_{C_{10}TAB} = 0.0340$ mol kg^{-1}) at 25 °C.

TABLE 2: EPR Parameters of CP^- (1.0×10^{-4} mol kg^{-1}) Measured at 25 °C in Heavy Water, in the PVA Aqueous Solutions, and in Swollen PVA Hydrogel

	A_N (G)	$\tau_C \times 10^{12}$ (s)
heavy water	16.24 ± 0.02	4.2 ± 0.4
PVA 1% w/w	16.24 ± 0.02	4.2 ± 0.4
PVA 2.5% w/w	16.23 ± 0.02	5.1 ± 0.5
PVA 4% w/w	16.23 ± 0.02	5.5 ± 0.5
PVA 10% w/w	16.23 ± 0.02	8.1 ± 0.8
PVA 14% w/w	16.20 ± 0.02	9.9 ± 1.0
PVA 16% w/w	16.18 ± 0.02	14.5 ± 1.4
PVA 18% w/w	16.18 ± 0.02	16.0 ± 1.6
PVA hydrogel	16.21 ± 0.02	7.6 ± 0.8

PVA concentration, see also Figure 2. These results indicate that CP^- is located in the polymer-poor domains of the cryogel, where it experiences a local viscosity lower than that experienced in concentrated PVA solutions, but still significantly higher than that found in pure water. Actually, the τ_C values of CP^- in the rehydrated gel patch is the same as that measured for an homogeneous solution containing ~9% w/w PVA (Figure 2). This result deserves further speculation: it is generally accepted that, in PVA cryogels, the polymer-poor phase, which constitutes more than 70% w/w of the whole hydrogel sample,[15] is a very dilute polymer solution. Consequently, it would be reasonable to expect the local environment experienced by CP^- in PVA hydrogels would be similar to that found in water. That this is not confirmed by the EPR results will be discussed below.

Concerning the study of the C_{10}TAB self-association in PVA hydrogel, the A_N and τ_C of CP^- measured on PVA patches rehydrated in C_{10}TAB solutions are reported in Figures 3 and 4 as a function of the surfactant molality, $m_{C_{10}TAB}$. Both parameters show an abrupt change at an $m_{C_{10}TAB}$ value at which

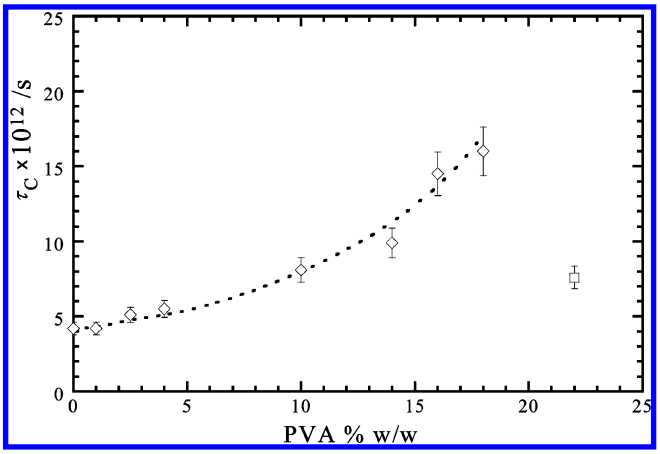

Figure 2. Rotational correlation time, τ_C, of CP^- in PVA liquid mixtures (◇, dotted line) and in PVA hydrogel (□), as a function polymer weight percent, at 25 °C.

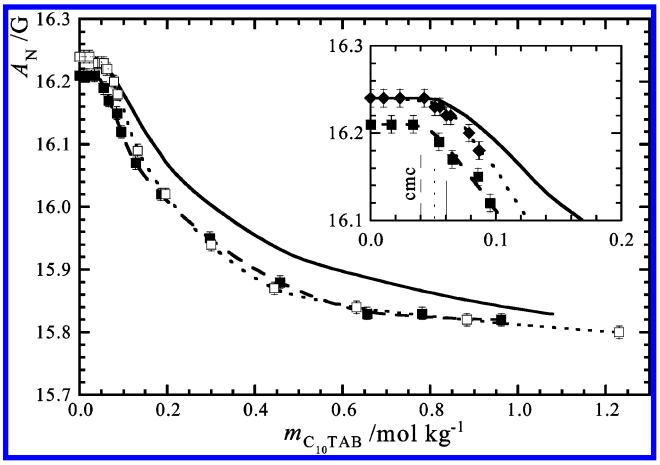

Figure 3. Nitrogen hyperfine coupling constant, A_N, of CP^- in PVA hydrogel (■, dashed line) and in PVA 1% w/w liquid mixtures (□, dotted line), as a function of C_{10}TAB molality, $m_{C_{10}TAB}$, at 25 °C. The continuous line shows the trend of A_N in water−C_{10}TAB mixtures. The insert shows the data in the dilute molality range.

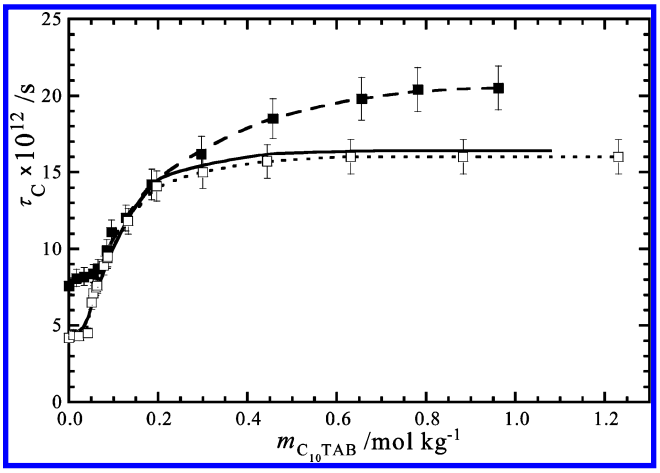

Figure 4. Rotational correlation time, τ_C, of CP^- in PVA hydrogel (■, dashed line) and in PVA 1% w/w liquid mixtures (□, dotted line), as a function of C_{10}TAB molality, $m_{C_{10}TAB}$, at 25 °C. The continuous line shows the trend of τ_C in water−C_{10}TAB mixtures.

the surfactant molecules start to self-aggregate, allowing the determination of the cmc (0.045 mol kg^{-1}). The variation of the spectroscopic parameters with increasing surfactant molality can be explained in terms of the physicochemical properties of CP^- solubilization site and/or the specific interaction it can have

TABLE 3: Critical Micellar Cncentration, cmc, of C_{10}TAB and CP^- EPR parameters in the Systems Water−C_{10}TAB, Water−C_{10}TAB−PVA (1% w/w), and in Hydrogel of PVA−C_{10}TAB

	cmc (mol kg^{-1})	A_N^{Ma} (G)	$K_d{}^b$	$\tau_C^M \times 10^{12c}$ (s)
water−C_{10}TAB[d]	0.060	15.69 ± 0.01	166 ± 7	16.0 ± 1.6
water−C_{10}TAB−PVA (1% w/w)	0.050	15.70 ± 0.02	250 ± 30	16.0 ± 1.6
hydrogel of PVA−C_{10}TAB	0.045	15.70 ± 0.02	220 ± 20	18.2 ± 1.8

[a] Nitrogen isotropic hyperfine coupling constant of CP^- solubilized in C_{10}TAB micelles formed in water, in PVA (1% w/w) aqueous solution, and in PVA hydrogel, calculated by eq 5 in the text. [b] Distribution coefficient of CP^- between aqueous and C_{10}TAB micellar pseudophases in water, PVA (1% w/w) aqueous solution, and PVA hydrogel, calculated by eq 5 in the text. [c] CP^- correlation time measured at higher C_{10}TAB concentration ($m_{C_{10}TAB} \gg$ cmc) in water, in PVA (1% w/w) aqueous solution, and in PVA hydrogel. [d] Data from ref 34.

with surfactant monomers and eventual micellar aggregates. In the premicellar composition range, A_N and τ_C are almost constant, assuming values remarkably close to those measured in the absence of C_{10}TAB. This evidence indicates no CP^-−monomeric surfactant interaction. In the micellar composition range, τ_C increases, indicating a restriction of the spin-probe rotational motion. Furthermore, A_N decreases, indicating that the CP^- NO moiety is positioned in a progressively less polar environment. This suggests that CP^- acts as a counterion to the C_{10}TAB micelles formed in the PVA hydrogel, condensing at the micelle−water interface, with its NO moiety oriented toward the micellar hydrophobic core.[34]

In Figures 3 and 4, the A_N and τ_C values of CP^- in PVA−C_{10}TAB hydrogels are compared with those in C_{10}TAB aqueous solutions. Furthermore, because the presence of polymers can strongly influence surfactant self-aggregation, as monitored by the EPR spin-probe approach, because of direct surfactant−polymer interactions,[38] some water−C_{10}TAB−PVA (1% w/w) mixtures were also investigated and the data are reported in the same figures. Overall, the trends of the EPR parameters are almost the same in all three systems and, in particular, the A_N curves overlay. This indicates that the C_{10}TAB micelles formed in the PVA hydrogel and in the PVA solution present the same hydrophobicity as those formed in pure water. The τ_C curve in the PVA solution (1% w/w) overlays that in water, while the τ_C trend in the PVA hydrogel is simply shifted to higher value. This is a further confirmation that the polymer-poor domains, in which surfactant molecules are located, are more viscous, i.e., contain more PVA, than expected.

The EPR results indicate the absence of any direct interaction between PVA and C_{10}TAB molecules, both as monomers and as micelles, in agreement with the literature reporting low or even negligible affinity between cationic surfactants and water-soluble neutral polymers.[24] Furthermore, it seems that C_{10}TAB micellization in the PVA hydrogel pores is similar to that in water. Actually, a deeper analysis of Figure 3 shows that the C_{10}TAB cmc slightly decreases in PVA solutions and decreases even more in PVA hydrogel, see Table 3. This could be related to the effectively increased surfactant concentration due to the excluded volume of the PVA.

In all the micellar systems considered, the interaction between the spin-probe and C_{10}TAB micelles can be quantitatively described by defining the CP^- distribution coefficient between the micelles and the aqueous environment:[39]

$$K_d = \frac{n^M_{CP^-}/n^M}{n^W_{CP^-}/n^W} \tag{3}$$

where $n^W_{CP^-}$ and $n^M_{CP^-}$ represent the moles of CP^- in the aqueous and in the micellar medium, respectively; n^W is the number of water moles and n^M is the number of moles of micellized surfactant (on the molality scale and using heavy water as solvent, $n^W = 50$ and $n^M = m_{C_{10}TAB}$ − cmc). The CP^- molality is low enough to ensure less than one spin-probe molecule can interact per micellar aggregate, thus avoiding spin-exchange between different CP^- molecules. Furthermore, the EPR spectra registered in all the samples under consideration show only three narrow lines, indicating that the CP^- exchange rate between the micelles and the aqueous medium is very high with respect to the separation (in frequency units) between the EPR lines in the two sites.[40] Consequently the experimental EPR spectrum is a weighed average of the signals due to spin-probes in different environments. In these conditions, the A_N values evaluated in micellar solution are an average between the nitrogen hyperfine coupling constant of CP^- molecules localized in the aqueous bulk, A^W_N, and that of CP^- interacting with the micelles, A^M_N, weighted in proportion to the relative spin-probe populations:

$$A_N = \frac{n^W_{CP^-}}{n_{CP^-}} A^W_N + \frac{n^M_{CP^-}}{n_{CP^-}} A^M_N \tag{4}$$

By substituting eq 3 into eq 4, one obtains:[31,39]

$$A_N = \frac{(A^M_N - A^W_N)\cdot K_d}{K_d + \frac{n^W}{n^M}} + A^W_N \tag{5}$$

Consequently, by assuming A^W_N equal to the value measured in the premicellar range, the fitting of eq 5 to the experimental data allows the evaluation of the K_d and A^M_N values. The K_d and A^M_N values obtained in water, PVA aqueous solutions, and PVA hydrogel are collected in Table 3. The A^M_N values are almost the same in all the considered systems, and the K_d values are quite similar, confirming that the micelles formed in the hydrogel pores present the same properties as those formed in PVA liquid solutions and in bulk water.

SANS Data. Some initial SANS cross sections, $d\Sigma/d\Omega$ vs Q, are shown in Figure 5 for the binary system heavy water−C_{10}TAB at three concentrations. The broad maximum in $d\Sigma/d\Omega$ is characteristic of charged micellar systems, where significant correlations between the micelles are present. Furthermore, the position of the correlation peak changes linearly with $m_{C_{10}TAB}{}^{1/3}$, as expected for charged micelles.[41]

Quantitative structural information on the aggregates in solution can be gained by an appropriate analysis of the experimental data.[42] The general scattering cross section, containing information about shape, size, and interactions of monodisperse scattering bodies, is given by

$$\frac{d\Sigma}{d\Omega} = N_b\left(\sum_i b_i - V_b\rho_s\right)^2 P(Q)S(Q) + \left(\frac{d\Sigma}{d\Omega}\right)_{inc} \tag{6}$$

where N_b is the number density of scattering bodies, V_b is the volume of each scattering body, $\sum_i b_i$ is the sum of the scattering

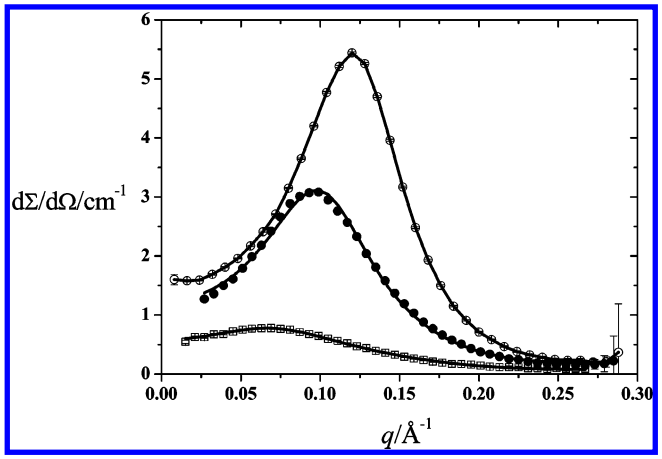

Figure 5. SANS data for $C_{10}TAB-D_2O$ solutions (cmc = 0.06 mol kg^{-1}) with surfactant concentration 0.101 mol kg^{-1} (□), 0.301 mol kg^{-1} (●), and 0.799 mol kg^{-1} (○) at 25 °C. Solid lines are fitting of eq 6 to the experimental data.

lengths over the atoms constituting the body, and ρ_s is the solvent scattering length density. $P(Q)$ and $S(Q)$ are the form and structure factors, respectively, while $(d\Sigma/d\Omega)_{inc}$ is the incoherent scattering cross section. The form factor contains information on the shape of the scattering objects, whereas the structure factor accounts for interparticle correlations and is normally observed for concentrated or charged systems. Equation 6 is generally expressed as an approximation, neglecting the effect of any preferred orientational alignment among anisotropic particles.

Structural parameters of pure $C_{10}TAB$ micelles were established by modeling the micellar aggregates as charged prolate ellipsoids and analyzing the scattering data through eq 6, where the number density of scattering bodies has been imposed to be $N_b = (m_{C_{10}TAB} - \text{cmc})L_A/N_{agg}$, with N_{agg} the aggregation number of the micelles, and L_A the Avogadro constant.

For a prolate ellipsoid the form factor $P(Q)$ is

$$P(Q) = \int_0^1 |F(Q,\mu)|^2 \, d\mu \tag{7}$$

whereas $S(Q)$, the orientationally averaged interparticle structure factor, is given by

$$S(Q) = 1 + \frac{|\int_0^1 F(Q,\mu)\, d\mu|^2}{\int_0^1 |F(Q,\mu)|^2 \, d\mu}(S_{MM}(Q) - 1) \tag{8}$$

In the above equations, $F(Q,\mu)$ is the angle-dependent form factor for ellipsoidal two-shell micelles, where μ is the direction cosine between the direction of the symmetry axis of the ellipsoid and the $\bar{Q}$ vector.

The micelle−micelle structure factor $S_{MM}(Q)$ can be derived on the basis of the interparticle interaction potential. A suitable choice to evaluate $S_{MM}(Q)$ for the binary system heavy water−$C_{10}TAB$ is the rescaled mean spherical approximation (RMSA), which is well described in the literature.[43,44]

Equation 6 can be fitted to the experimental scattering cross section distributions with N_{agg}, z (the actual micelle charge) and d (the thickness of the micelle hydrophilic shell, formed by the polar heads, counterions, and hydration water molecules, which are n_w per head) as unknown parameters.[42] The length of the short axis of the ellipsoidal micellar hydrophobic core, b, has been taken equal to the length of a fully extended alkyl chain, computed according to the Tanford studies.[45] The length of the long axis, a, has been computed assuming a close-packed core.[42] The fits are shown in Figure 5, while the extracted parameter are reported in Table 4. In the concentration range explored here, the fitted parameters of the micellar form factor do not substantially vary, so there is no significant growth of the C_{10}-TAB micelle with concentration. The differences in the experimental scattering patterns are caused by an increase in correlation as the volume fraction of charged scattering objects increases.

TABLE 4: Structural Data Obtained from SANS Measurements for $C_{10}TAB$ Micelles in Heavy Water at 25 °C

$m_{C_{10}TAB}$ (mol kg^{-1})	a[a] (Å)	b[b] (Å)	d[c] (Å)	N_{aggr}[d]	z[e]	n_w[f]
0.101	15.3	14.1	2 ± 1	46 ± 2	19 ± 2	10 ± 2
0.301	17.0	14.1	7 ± 2	51 ± 2	13 ± 6	14 ± 2
0.542	17.7	14.1	4 ± 2	56 ± 3	18 ± 4	10 ± 4

[a] Length of the ellipsoidal micelle long axis. [b] Length of the short axis of the ellipsoidal micellar hydrophobic core. [c] Thickness of the micelle hydrophilic shell. [d] Aggregation number. [e] Actual micelle charge. [f] Hydration water molecules per surfactant headgroup.

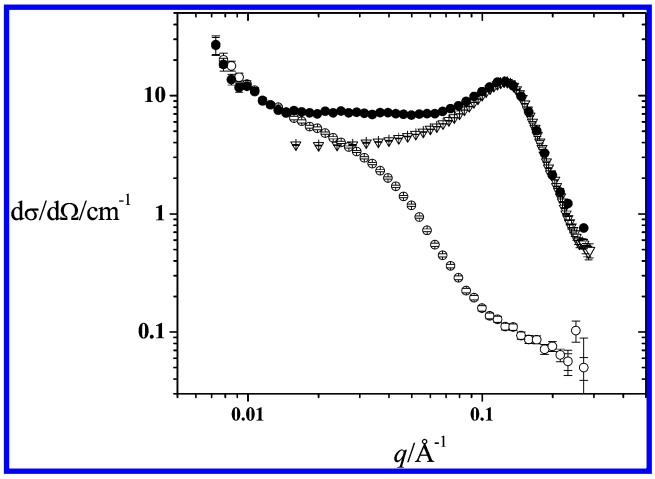

Figure 6. SANS data of the PVA hydrogel (○), $C_{10}TAB-D_2O$ solution (▽), and $C_{10}TAB$-containing hydrogel (●) measured at 25 °C ($m_{C_{10}TAB}$ = 0.799 mol kg^{-1}, cmc = 0.06 mol kg^{-1}).

The results of a SANS characterization of the PVA freeze/thaw hydrogel performed by some of us have been recently reported in the literature.[16,17] It has been shown that freeze/thaw PVA hydrogels are characterized, from a mesoscopic point of view, by polymer-rich domains, whose mean extension is of the order of 1−1.5 μm, delimiting water-rich pores. From a microscopic point of view, the polymer-rich phase is constituted by a swollen network in which polymer chains are physically tangled, forming crystalline cross-linking points (crystallites), whose radius is found to be around ∼40 Å, interconnected by amorphous chains.

The scattering cross section distribution of a $C_{10}TAB$-containing hydrogel sample ($m_{C_{10}TAB}$ = 0.799 mol kg^{-1}) is reported in Figure 6, where it is compared to the curve of the surfactant-free hydrogel sample and to the heavy water−C_{10}-TAB aqueous solution at the same surfactant concentration. It is apparent that, at low Q values (0.007−0.015 Å), the curve of the $C_{10}TAB$-containing hydrogel sample overlaps that of the surfactant-free PVA hydrogel; particularly, $I(Q) \propto Q^{-D}$ with $D \sim 3$ for both curves. This suggests that the nature of the polymer-rich phase is quite insensitive to the presence $C_{10}TAB$ micelles.

At moderate and high Q values, the scattering profile of the $C_{10}TAB$-containing hydrogel sample results markedly different

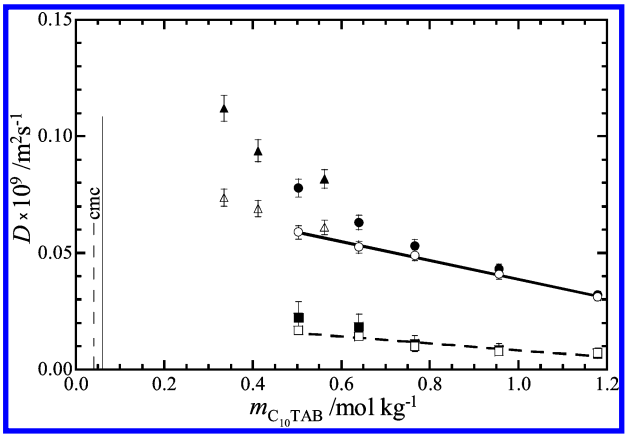

Figure 7. Intradiffusion coefficients of $C_{10}TAB$ and hydrophobic molecular probes located in the micelles as a function of the surfactant molality, $m_{C_{10}TAB}$, at 25 °C. $D^{W}_{C_{10}TAB}$ (●) and $D^{W}_{C_{10}TAB,M}$ (○, apolar probe HMDSO, continuous line) in aqueous solutions, present work. $D^{W}_{C_{10}TAB}$ (▲) and $D^{W}_{C_{10}TAB,M}$ (△, apolar probe TMS) in aqueous solutions, ref 50. $D^{gel}_{C_{10}TAB}$ (■) and $D^{gel}_{C_{10}TAB,M}$ (□, apolar probe HMDSO, dashed line) in PVA hydrogel, present work. The continuous and dashed vertical lines indicate the cmc in water and PVA hydrogel, as obtained by EPR measurements.

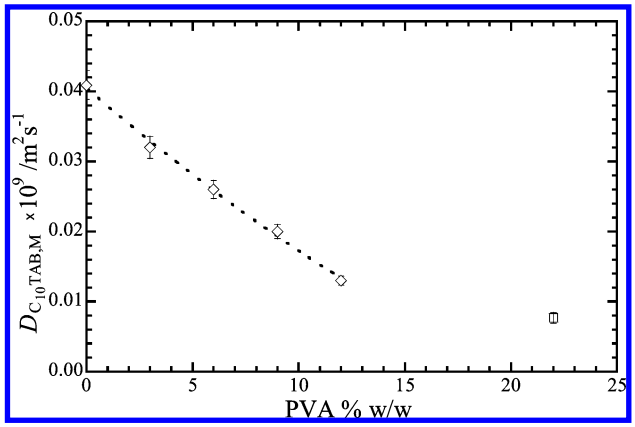

Figure 8. $C_{10}TAB$ intradiffusion coefficient as a function of the PVA concentration, at 25 °C in water solution (◇) and in the PVA hydrogel ($m_{C10TAB} = 0.956$ mol kg^{-1}) (□). The PVA content in the hydrogel is ∼22% w/w.

with respect to that of the pure PVA gel. The shoulder observed for the hydrogel disappears completely when $C_{10}TAB$ is added to the gel. Furthermore, the $C_{10}TAB$-containing hydrogel sample shows a correlation peak that reflects the presence of the surfactant micelles at $Q \sim 0.012$ Å. The position and magnitude of such a peak is nearly equal to that observed for the pure $C_{10}TAB-D_2O$ system, see Figure 6. This experimental evidence strongly suggests that the number and the structural parameters of micelles, present in the gel, are similar to those of the micelles present in the corresponding $C_{10}TAB-D_2O$ binary system. Overall, the SANS evidence indicates scarcely any interaction between the PVA chain of the gel matrix and the $C_{10}TAB$ in the aggregate or free form, supporting what was already inferred from EPR data.

^{1}H PGSE-NMR Data. The information obtained by PGSE-^{1}H NMR measurements is remarkably important in carrier and delivery processes.[46,47] For the basic characterization of polymeric hydrogel samples, this technique gives information on: (i) the interaction between diffusing molecules and the polymer chains[48] and (ii) the hydrogel structure as this determines the properties of the medium in which diffusion occurs and the path followed by the diffusing molecules.[49]

In the present work, the intradiffusion coefficients of $C_{10}TAB$ in PVA hydrogel, $D^{gel}_{C_{10}TAB}$, and in heavy water, $D^{W}_{C_{10}TAB}$, were determined by following the decay of the NMR peak of the methyl groups on the headgroup of $C_{10}TAB$ (chemical shift = 3.2) as a function of the square of the gradient strength, G^2. In all cases, a monoexponential decay was observed, indicating that only one diffusing species is present in the systems or that the exchange of the molecules between the local environment in which their mobility is different is fast with respect to the experimental observation time ($\Delta = 0.1$ s). The $C_{10}TAB$ intradiffusion coefficients measured in PVA cryogel and in water are shown in Figure 7. In these systems, surfactant molecules are present both as free monomers and as micellar aggregates, the experimental intradiffusion coefficient being a mean value between that of the two species. The intradiffusion coefficient of micelles both in hydrogel, $D^{gel}_{C_{10}TAB,M}$, and in water, $D^{W}_{C_{10}TAB,M}$, can be measured by the addition of an apolar probe, a compound which is entirely confined to the micelles and has a negligible solubility in the aqueous medium. An ideal probe will perturb the micelle as little as possible. For spherical and relatively small micelles, tetramethylsilane (TMS) is generally preferred,[50,51] although its low boiling point requires some care in sample preparation. This probe was employed in the previous study on $C_{10}TAB$ micellization in aqueous solution,[50] whose data are also shown in Figure 7. In the present work, hexamethyldisiloxane (HMDSO) was preferred. This probe is more bulky and asymmetric but is less volatile, which makes sample preparation easier. Inspection of Figure 7 shows that the data obtained in aqueous solution using HMDSO and TMS are in very good agreement, indicating that the micelle structure is not evidently perturbed by the HMDSO insertion. Furthermore, $D^{gel}_{C_{10}TAB,M}$ and $D^{W}_{C_{10}TAB,M}$ are only slightly lower than $D^{gel}_{C_{10}TAB}$ and $D^{W}_{C_{10}TAB}$, respectively; this evidence indicates that, because the measurements have been performed at surfactant molalities much higher than the cmc, the contribution of the surfactant monomers to the experimental intradiffusion coefficient is low.

The most obvious finding of the PGSE-NMR investigation is that diffusion of $C_{10}TAB$ micelles in PVA hydrogels ($D^{gel}_{C_{10}TAB,M}$) is much slower than in bulk heavy water ($D^{W}_{C_{10}TAB,M}$) (Figure 7). This experimental evidence cannot be ascribed to the occurrence of some direct interaction between surfactant molecules and polymeric chains because EPR and SANS measurements have indicated that the formation of micelles is not influenced by the presence of polymer chains, both in solution and in the gel. The low value of intradiffusion coefficient of micelles in the gel, instead, is probably due to the intrinsic structural features of freeze/thaw PVA hydrogel. Diffusion of $C_{10}TAB$ micelles in freeze/thaw PVA hydrogels is expected to occur primarily within the pores delimited by the polymer-rich phase, which contain the polymer-poor phase that, as indicated by our EPR analysis, is a PVA aqueous water solution with concentration ∼9% w/w. Consequently, micelle mobility within the gel can be affected by: (i) restriction in confined environment and (ii) medium viscosity as determined by the presence of PVA chains. To quantitatively analyze the relevance of these two factors, both of which lead to a decrease of micelle mobility, we have determined the $C_{10}TAB$ micelle intradiffusion coefficient in heavy water−PVA mixtures ($D^{sol}_{C_{10}TAB,M}$) with polymer concentration ranging from 3 to 12% w/w at a fixed surfactant molality ($m_{C10TAB} = 0.956$ mol kg^{-1}). Inspection of Figure 8 shows that micelle mobility in a 9% w/w PVA aqueous solution is higher than that measured in the gel, particularly $D^{gel}_{C_{10}TAB,M}/D^{sol}_{C_{10}TAB,M} = 0.38 \pm 0.02$. In the as-

sumption that micelles are located in the polymer-poor regions and that the PVA concentration in this region is ~9% w/w, as obtained by EPR data, the lower value of micellar intradiffusion in the gel with respect to that in a 9% w/w polymer solution can be interpreted as a reflection of micelle restriction within the pores.

Some indications on the pore dimensions could be obtained by analyzing the experimental intradiffusion data in the framework of hydrodynamic models from the literature. Several papers have been published that address the topic of hindered diffusion in a hydrogel.[52−58] Particularly, Phillips, combining elements of previously reported studies, derived a specific model concerning diffusion of micelles in a hydrogel.[54] Such models have been tailored for hydrogels whose scaffold is formed by single polymer chains, modeled as thin cylinders, joining the different cross-links. However, these models are not descriptive of hydrogels, such as PVA cryogels, in which the scaffold is formed by semicrystalline polymer-rich domains with dimensions much larger than that of the diffusing particle. In this case, among those present in the literature, we think that a more appropriate model is that proposed by Coffman and co-workers[59] concerning protein diffusion in porous chromatographic media. Diffusion in a porous medium potentially has contributions from both hydrodynamic hindrance and tortuosity. The hydrodynamic hindrance of pore walls on the particle mobility is represented by a factor K_D (≤ 1), which is a function of $\lambda = r_s/R_{pore}$, i.e., the ratio of the particle radius, to that of the pore. Anderson and Quinn derived a semiempirical correlation, which holds for $\lambda < 0.4$:[60]

$$K_D = 1 - 2.1044\,\lambda + 2.089\,\lambda^3 - 0.948\,\lambda^5 \qquad (9)$$

The effect of tortuosity is represented by a tortuosity factor κ, whose value is 2 for isotropic porous media. The diffusivity of the solute within the network of interconnected pores, D^{pore}, is related to the solution diffusivity, D^{sol}, by the relation:

$$\frac{D^{pore}}{D^{sol}} = \frac{1}{\kappa K_D} \qquad (10)$$

The pore diffusivity is related to the experimental intradiffusion coefficient in the gel as follows:

$$D^{gel} = \epsilon^{pore}\, D^{pore} \qquad (11)$$

where ϵ^{pore} is the gel volume fraction accessible to diffusing particles.

In the case of our gel, ϵ^{pore} can be assumed equal to the volume fraction occupied by the polymer-poor phase, which constitutes ~70% of the gel samples.[15] By combining eqs 9−11 and using our experimental intradiffusion coefficients ($D^{gel}/D^{sol} = D^{gel}_{C_{10}TAB,M}/D^{sol}_{C_{10}TAB,M} = 0.38 \pm 0.02$), it is possible to estimate that the mean radius of macropores in PVA cryogel is ~0.1 μm, confirming the order of magnitude derived from rheological measurements.[19]

PVA Cryogel Microstructure. Our experimental evidence prompts speculation on the local environment experienced by molecules solubilized in the PVA cryogel. Particularly, the rotational motion of the spin-probe CP^- and the translational motion of $C_{10}TAB$ micelles, measured using independent experimental techniques such as EPR and PGSE-NMR, respectively, give concordant information on the local environment of the host system. Guest molecules may reasonably be supposed to be incorporated in the polymer-poor phase, which is confined in interconnected macropores embedded in the network scaffolding. EPR experiments indicated that the spin-probe and micelles present in the gel experience a local environment equivalent to that one of a solution with an average of ~9% w/w PVA, and therefore that the polymer-poor phase is not a highly diluted PVA solution. Because the polymer-poor phase constitutes ~70% w/w of the whole hydrogel sample,[15] this allows the concentration of PVA in the polymer-rich phase to be estimated as ~52% w/w (in heavy water). Furthermore, the reduced translational dynamics of micelles inside the gel has been interpreted as due to their restriction in the polymer-poor macropores, for which models[59] borrowed from protein diffusion suggest an average dimension of ~0.1 μm.

The quite surprising result that the PVA concentration in the polymer-poor domains is not negligible may throw light on the formation of freeze/thaw hydrogels. Freeze/thaw PVA hydrogels are nonequilibrium systems which undergo continuous, but slow, syneresis even if they are preserved at room temperature in controlled conditions. According to this mechanism, the formation of freeze/thaw PVA hydrogels is the result of competing thermodynamic and kinetic effects. The initial homogeneous solutions already form a gel during the first freeze/ thaw cycle. On the basis of equilibrium thermodynamic data, the initial homogeneous solution should undergo spinodal decomposition at −20 °C, i.e., at the hydrogel freezing temperature, giving rise to a polymer-poor phase, which is generally supposed to be an extremely diluted aqueous polymer solution, practically heavy water.[61] However, because the freezing procedure is quite fast, the formation of ice crystals may easily inhibit the spinodal decomposition so that the phase separation in polymer-rich and polymer-poor regions is either not complete or quite suppressed. This means that the polymer-poor phase could contain more polymer than expected. Furthermore, it is also possible that when the sample is thawed, the amorphous fraction of the polymer-rich phase is partially redissolved in the pores. In other words, the polymer-poor phase becomes more concentrated than expected based on thermodynamic data. Also, because many polymer chain portions acting as tie chains between the microcrystallites are at the same time partially dissolved in the pores, their motion is strongly reduced. Consequently, the dynamics of guest molecules in the gels is significantly more hindered than in bulk water and similar to that of a liquid polymer solution more concentrated in PVA. In this context, it is interesting to note that water intradiffusion within PVA hydrogels[19,62] is also found to be lower than expected. In a recent ^{17}O NMR investigation,[63] it was additionally found that the water molecules in PVA hydrogel are more structured than in bulk water, i.e., an increase in the number of hydrogen bonds and a decrease of the hydrogen-bond length occur. This evidence, which could be connected with a solvent structuring effect of PVA, further enhanced by the gelation process, supports the hypothesis that, within the polymer-poor phase of PVA hydrogel, all the dynamic processes are slowed.

Conclusions

This work has provided a wide experimental characterization of $C_{10}TAB$ self-aggregation in PVA hydrogels. The combined experimental strategy, including EPR, SANS, and PGSE-NMR, is a valuable contribution to the study of such interesting systems as surfactant-containing hydrogel formulations and can be fruitfully employed in other cases. Overall, the experimental results presented in this work have shown that $C_{10}TAB$ micellization is almost unperturbed by the confinement of the surfactant molecules within the polymeric network of a freeze/thaw PVA hydrogel, no direct surfactant−polymer interaction taking place.

From an applicative viewpoint, the results of the present work indicate that surfactant-containing PVA hydrogels present a complex multidomain structure able to host both hydrophilic and hydrophobic guest molecules. Furthermore, diffusion of the guest molecules is quite slow. Consequently, these systems, or similar ones with a suitable, nontoxic surfactant, seem quite promising for the design of new materials for controlled release and/or adsorption of host molecules.

Acknowledgment. The Centro di Competenza "Nuove Tecnologie per le Attivita Produttive" Regione Campania P.O.R. 2000-2006 Misura 3.16 is gratefully acknoweledged for financial support. We thank Prof. Lucia Costantino and Prof. Ornella Ortona for their helpful comments. We thank Rutherford Appleton Laboratory for provision of beam time.

References and Notes

(1) Mandal, T. K.; Bostanian, L. A.; Graves, R. A.; Chapman, S. R. *Pharm. Res.* **2002**, *19*, 1713−1719.
(2) Fu, J.; Fiegel, J.; Krauland, E.; Hanes, J. *Biomaterials* **2002**, *23*, 4425−4433.
(3) Peppas, N. A.; Tennenhouse, D *J. Drug Delivery Sci. Technol.* **2004**, *14*, 291−297.
(4) Fernandez Degiorgi, C.; Pizarro, R. A.; Smolko, E. E.; Lora, S.; Carenza, M. *Radiat. Phys. Chem.* **2002**, *63*, 109−113.
(5) Peppas, N. A.; Mongia, N. K. *Eur. J. Pharmacol. Biopharm.* **1997**, *43*, 51−58.
(6) Urushizaki, F.; Yamaguchi, H.; Nakamura, K.; Numajiri, S.; Sugibayashi, K.; Morimoto, Y. *Int. J. Pharm.* **1990**, *58*, 135−142.
(7) Mori, Y.; Tokura, H.; Yoshikawa, M. *J. Mater. Sci.* **1997**, *32*, 491−496.
(8) Hassan, C. M.; Peppas, N. A. *Adv. Polym. Sci.* **2000**, *153*, 37−65.
(9) Lozinsky, V. I. *Russ. Chem. Rev.* **2002**, *71*, 489−511.
(10) Peppas, N. A.; Simmons, R. E. P. *J. Drug Delivery Sci. Technol.* **2004**, *14*, 285−289.
(11) Wan, W. K.; Campbell, G.; Zhang, Z. F.; Hui, A. J.; Boughner, D. R. *J. Appl. Polym. Sci.* **2002**, *51*, 2041−2046.
(12) Hyon, S. H.; Cha, W. I.; Ikada, Y.; Kita, M.; Ogura, Y.; Honda, Y. *J. Biomater. Sci., Polymer Ed.* **1994**, *5*, 397−406.
(13) Peppas, N. A. *Makromol. Chem.* **1975**, *176*, 3433−3440.
(14) Yokoyama, F.; Masada, I.; Shimamura, K.; Ikawa, T.; Monobe, K. *Colloid Polym. Sci.* **1986**, *264*, 595−601.
(15) Ricciardi, R.; Auriemma, F.; De Rosa, C.; Lauprêtre, F. *Macromolecules* **2004**, *37*, 1921−1927.
(16) Mangiapia, G.; Ricciardi, R.; Auriemma, F.; Lo Celso, F.; Heenan, R. K.; D'Errico, G.; Paduano, L. *J. Phys. Chem. B*, submitted.
(17) Ricciardi, R.; Mangiapia, G.; Lo Celso, F.; Paduano, L.; Triolo, R.; Auriemma, F.; De Rosa, C.; Lauprêtre, F. *Chem. Mater.* **2005**, *17*, 1183−1189.
(18) Ricciardi, R.; Auriemma, F.; Gaillet, C.; De Rosa, C.; Lauprêtre, F. *Macromolecules* **2004**, *37*, 9510−9516.
(19) Ricciardi, R.; D'Errico, G.; Auriemma, F.; Ducouret, G.; Tedeschi, A. M.; De Rosa, C.; Lauprêtre, F.; Lafuma, F. *Macromolecules* **2005**, *38*, 6629−6639.
(20) Hassan, C. M.; Peppas, N. A. *Adv. Polym. Sci.* **2000**, *153*, 37−65.
(21) Mandal, T. K.; Bostanian, L. A. *Pharm. Dev. Technol.* **2000**, *5*, 555−560.
(22) Morimoto, K.; Fukanoki, S.; Hatakeyama, Y.; Nagayasu, A.; Morisaka, K.; Hyon, S. H.; Ikada, Y. *J. Pharm. Pharmacol.* **1990**, *42*, 720−722.
(23) Hiemenz, P. C. *Principles of Colloids Surface Chemistry*; Marcel Dekker: New York, 1986.
(24) Kwak, J. C. T. *Polymer-Surfactant Systems*; Marcel Dekker: New York, 1998.
(25) Weiss, J. *Handbook of Ion Chromatography*; Wiley-VCH: Weinheim, 2004.
(26) Saracino, G. A. A.; Tedeschi, A.; D'Errico, G.; Improta, R.; Franco, L.; Ruzzi, M.; Corvaia, C.; Barone, V. *J. Phys. Chem. A* **2002**, *106*, 10700−10706.
(27) Heenan, R. K.; Penfold, J.; King, S. M. *J. Appl. Crystallogr.* **1997**, *30*, 1140−1147.
(28) Stilbs, P. *Prog. NMR Spectrosc.* **1987**, *19*, 1−45.
(29) Bales, B. L.; Zana, R. *J. Phys. Chem. B* **2002**, *106*, 1926−1939.
(30) Ottaviani, M. F.; Andechaga, P.; Turro, N. J.; Tomalia, D. A. *J. Phys. Chem. B* **1997**, *101*, 6057−6065.
(31) Rizzi, C.; Mathieu, C.; Tuccio, B.; Lauricella, R.; Boutellier, C.; Tordo P. *J. Chem. Soc., Perkin Trans. 2* **1999**, 2777−2781.
(32) Wasserman, A. M.; Kasaikin, V. A.; Zakharova, Y. A.; Aliev, I. I.; Baranovsky, V. Y.; Doseva, V.; Yasina, L. L. *Spectrochim. Acta, Part A* **2002**, *58*, 1241−1255.
(33) Windle, J. J.; Scherrer, R. *Magn. Reson. Chem.* **1992**, *30*, 927−939.
(34) Tedeschi, A.; D'Errico, G.; Franco, L.; Ruzzi, M.; Corvaia, C. *Phys. Chem. Chem. Phys.* **2003**, *5*, 4204−4209.
(35) Kivelson, D. *J. Chem. Phys.* **1960**, *33*, 1094−1106.
(36) Galantini, L.; D'Archivio, A.; Lora, S.; Corain, B. *J. Mol. Catal. B: Enzym.* **1999**, *6*, 505−508.
(37) Gillies, D. G.; Sutcliffe, L. H.; Wu, X.; Belton, P. S. *Food Chem.* **1996**, *55*, 349−352.
(38) Tedeschi, A. M.; Busi, E.; Paduano, L.; Basosi, R.; D'Errico, G. *Phys. Chem. Chem. Phys.* **2003**, *5*, 5077−5083.
(39) Rizzi, R. Lauricella, B. Tuccio, B.; Bouteiller, C.; Cerri, V.; Tordo, P. *J. Chem. Soc., Perkin Trans. 2* **1997**, 2507−2512.
(40) Jolicoeur, C.; Friedman, H. L. *J. Solution Chem.* **1978**, *7*, 813−835.
(41) Berr, S. S.; Jones, R. R. M. *J. Phys. Chem.* **1989**, *93*, 2555−2558.
(42) Mangiapia, G.; Berti, D.; Baglioni, P.; Teixeira, J.; Paduano, P. *J. Phys. Chem. B* **2004**, *108*, 9772−9779.
(43) Hayter, J. B.; Penfold, J. *Mol. Phys.* **1981**, *42*, 109−118.
(44) Hansen, J. P.; Hayter, J. B. *Mol. Phys.* **1982**, *64*, 651−656.
(45) Tanford, C. *J. Phys. Chem.* **1972**, *76*, 3020−3024.
(46) Momot, K. I.; Kuchel, P. W. *Concepts Magn. Reson., Part A* **2003**, *19*, 51−64.
(47) Shapiro, Y. E.; Pykhteeva, E. G.; Levashov, A. V. *J. Colloid Interface Sci.* **1998**, *206*, 168−176.
(48) Carlsson, A.; Karlstrom, G.; Lindman, B. *J. Phys. Chem.* **1989**, *93*, 3673−3677.
(49) Yasunaga, H.; Ando, I. *Polym. Gels Networks* **1993**, *1*, 267−274.
(50) D'Errico, G.; Ortona, O.; Paduano, L.; Vitagliano, V. *J. Colloid Interface Sci.* **2001**, *239*, 264−271.
(51) Annunziata, O.; Costantino, L.; D'Errico, G.; Paduano, L.; Vitagliano, V. *J. Colloid Interface Sci.* **1999**, *216*, 16−24.
(52) Valente, A. J. M.; Polishchuk, A. Y.; Lobo, V. M. M.; Burrows, H. D. *Langmuir* **2000**, *16*, 6475−6479.
(53) Valente, A. J. M.; Polishchuk, A. Y.; Burrows, H. D.; Miguel, M. G.; Lobo, V. M. M. *Eur. Polym. J.* **2003**, *39*, 1855−1865.
(54) Phillips, R. J. *Biophys. J.* **2000**, *79*, 3350−3353.
(55) Amsden, B. *Macromolecules* **1998**, *31*, 8382−8395.
(56) Clague, D. S.; Phillips, R. J. *Phys. Fluids.* **1996**, *8*, 1720−1731.
(57) Johansson, L.; Hedberg, P.; Löfroth, J. E. *J. Phys. Chem.* **1993**, *97*, 747−755.
(58) Johansson, L.; Löfroth, J. E. *J. Phys. Chem.* **1993**, *97*, 7471−7479.
(59) Coffman, J. L.; Lightfoot, E. N.; Root, T. W. *J. Phys. Chem. B* **1997**, *101*, 2218−2223.
(60) Anderson, J. L.; Quinn, J. A. *Biophys. J.* **1974**, *14*, 130−150.
(61) Willcox, P. J.; Howie, D. W. J. R.; Schimdt-Rohr, K.; Hoagland, A.; Gido, S. P.; Pudjijanto, S.; Kleiner, L. W.; Venkatraman, S. *J. Polym. Sci. B* **1999**, *37*, 3438−3454.
(62) Shapiro, Y. E. *Colloids Surf. A* **2000**, *164*, 71−83.
(63) Machida, Y.; Kuroki, S.; Kanekiyo, M.; Kobayashi, M.; Ando, I.; Amiya, S.; *J. Mol. Struct.* **2000**, *554*, 81−90.